Journal of Alloys and Compounds 509 (2011) 7134–7138

Contents lists available at ScienceDirect

Journal of Alloys and Compounds

journal homepage: www.elsevier.com/locate/jallcom

Unusual magnetic properties of NiO nanoparticles embedded in a silica matrix

Marin Tadić[a,*], Matjaž Panjan[b], Dragana Marković[a], Irena Milošević[c], Vojislav Spasojević[a]

[a] Condensed Matter Physics Laboratory, Vinca Institute, University of Belgrade, POB 522, 11001 Belgrade, Serbia
[b] Jožef Stefan Institute, Jamova 39, 1000 Ljubljana, Slovenia
[c] Laboratoire CSPBAT, UMR 7244 CNRS Université Paris 13, 93017 Bobigny Cedex, France

ARTICLE INFO

Article history:
Received 3 January 2011
Received in revised form 4 April 2011
Accepted 5 April 2011
Available online 9 April 2011

Keywords:
Nickel oxide (NiO)
Hysteresis loop
Nanomaterials
Sol–gel synthesis
Magnetic materials

ABSTRACT

We have observed unusual magnetic properties of NiO (nickel oxide) nanoparticles embedded in a silica matrix. The sample was synthesized by a method based on the contribution of sol–gel and combustion processes. X-ray powder diffraction (XRPD) of the sample shows the formation of the nanocrystalline NiO phase whereas transmission electron microscope (TEM) reveals spherical-shaped nanoparticles of about 4 nm diameter. Moreover, HRTEM images show lattice fringes of the nanoparticles and defects in the crystal structure. The temperature and field dependence of the magnetization are also measured. The zero-field-cooled (ZFC) measurements show two maximums, one sharp and narrow at low temperatures ~6.5 K and an other broad one at higher temperature ~64 K. The FC magnetization shows a continuous increase upon lowering the temperature. The M(H) measurements reveal that NiO nanoparticles display anomalous hysteretic behaviors at low temperatures (below the low temperature maximum in the ZFC curve, 2 K and 5 K) showing that the magnetization initial curve lies below the hysteresis loop for a certain field range. Moreover, jump of the magnetization at low temperatures (2 K and 5 K) are also observed. These features represent novel magnetic properties for nanosized NiO which may be attributed to the surface spins. Moreover, these results indicate that the NiO nanoparticle consists of magnetically disorder shell and antiferromagnetically order core with an uncompensated magnetic moment.

1. Introduction

In the last few years, antiferromagnetic nanosized systems and their preparation and investigation have been active research topics in materials science [1–8]. The nickel oxide (NiO) has attracted much attention and it has been used in magnetic devices, antibacterial applications, catalysis, electrode materials, sensors and electrical devices [9–17].

Bulk nickel oxide possesses antiferromagnetic characteristic with a Néel temperature of $T_N \approx 523$ K [18]. Its magnetic properties are very sensitive on the particle size and broad spectrum of magnetic properties has been obtained in the nanosized systems such as superparamagnetism, spin glass, high magnetization, high magnetic moment of the particles, high coercivity, high exchange bias, memory and aging effects [19–34]. Therefore, NiO magnetic properties arise from both the atoms which reside on the surface of the nanoparticles, and from the atoms in the nanoparticle crystalline core. The reported results have revealed that the surface spins may dominate on the magnetic properties of NiO nanoparticles at low temperatures where surface spins are frozen in the spin-glass-like configuration. Moreover, various theories and experimental results are reported to explain magnetic behavior of NiO nanoparticles but full understanding of the magnetic properties is still not complete. Kodama et al. reported a model where the spins in NiO nanoparticles yield multisublattice configuration, indicating that the reduced coordination of surface spins leads to an important change in the magnetic order of the whole particle [24]. Winkler et al. prepared NiO nanoparticles with high saturation magnetization $M_S \approx 65$ emu/g, freezing and blocking temperature, and huge magnetic moment of the particles $m_p \approx 500\ \mu_B$ [21,22]. Vaidya et al. synthesized NiO/SiO_2 core–shell nanostructures and studied dependence of magnetic susceptibility on the weight content of SiO_2 [29]. Jagodič et al. reported on surface-spin magnetism of antiferromagnetic NiO in both nanoparticle and bulk form [23]. Ge et al. reported monodispersed NiO nanoflowers with anomalous magnetic behavior below blocking temperature (cusps in the ZFC and FC curves at 21 K) which might be linked with uncompensated spins [27]. Moreover, a reduction of the Néel temperature with decreasing particle size has been also observed in NiO nanoparticles [35]. Particular attention has been paid to the synthesis of nanostructural nickel oxide materials to enhance their performance in applications and to better understand their properties. For those reasons, various techniques have been proposed in order to produce nanosized NiO such as sol–gel, anodic arc plasma, solvothermal, thermal decomposition, solid-state milling, chemical precipitation, hydrothermal, molten-salt

* Corresponding author.
E-mail address: marint@vinca.rs (M. Tadić).

0925-8388/$ – see front matter © 2011 Elsevier B.V. All rights reserved.
doi:10.1016/j.jallcom.2011.04.032

synthesis, and magnetron sputtering technique [36–48]. The preparation of magnetic nanoparticles embedded in a non-magnetic matrix has been very interesting for fundamental studies and applications. Among different matrixes silica is advanced because of its non-toxic nature, high biocompatibility, prevention of agglomeration, temperature resistance, chemical inertness and adjustable pore diameter [26,29,30,49–56]. Sol–gel method has been very useful for preparation of the nanoparticles in amorphous silica [49–51]. A sol–gel combustion method is also utilized in the synthesis of nanomaterials [30,57].

The aim of this work is to present a peculiar magnetic behavior of the NiO nanoparticles embedded in a silica matrix. The investigation of the sample shows phase purity of NiO nanocrystals, spherically shaped NiO nanoparticles of about 4 nm diameters, lattice fringes of the nanoparticles and crystal defects, as well as anomalous magnetic behavior (two maximums in the ZFC curve and hysteretic behavior where initial curve lies below hysteresis loop). The results show that the NiO nanoparticle consists of magnetically disorder shell and antiferromagnetically order core with an uncompensated magnetic moment. The possible explanations for the observed anomalous magnetic behavior may arise from the surface spins.

2. Experimental

The NiO nanoparticles embedded in a silica matrix were prepared by utilizing the sol–gel combustion method [30]. The synthesis process in this work was done at lower heating temperature ($T_{heating}$ = 300 °C) compared to our previously work ($T_{heating}$ = 500 °C).

The X-ray powder diffractometer (Phillips PW-1710) employing CuKα (λ = 1.5406 Å, 2θ = 10–70°) radiation was used to characterize the crystal structure of the nanocomposite (step 0.02°, exposition 20 s/step). The size, morphology and nanostructure were observed by SEM (scanning electron microscope, JEOL 840A) and TEM (transmission electron microscopy, JEOL 2010 F). The magnetic properties of the sample were performed using a commercial Quantum Design MPMS-XL-5 SQUID-based magnetometer in a wide range of temperatures (2–300 K) and applied DC fields (up to 5 T).

3. Results and discussion

The phase purity of the sample was examined by X-ray powder diffractometer. The recorded and indexed diffraction pattern is shown in Fig. 1(a) where broad peaks can be observed, as expected for a nanocrystalline sample. All diffraction peaks coincide with peaks characteristic of the NiO phase. The mean crystallite diameter D was estimated using Scherrer's equation ($D \approx 0.9\lambda/\beta \cos\theta$) and the (2 0 0) reflection. We obtained a value of $D \approx 3.7$ nm. The silica matrix is in an amorphous state (broad peak around $2\theta \approx 22°$). The low-magnification SEM image (Fig. 1(b)) shows that the sample is made of big grains of the NiO/SiO_2 nanocomposite (few micrometers). The SEM image shows the appearance and size of NiO/SiO_2 grains whereas TEM measurements were performed for the purpose of examining NiO nanoparticles (their morphology, nanoparticle size and nanostructure).

Fig. 2 shows TEM images of the sample. TEM images show that the grains consist of spherically shaped nanoparticles that are embedded in an amorphous matrix. Moreover, the nanoparticles are well dispersed in the matrix. The figures also show that the particle size distribution is narrow with an average size of about 4 nm. We notice that the average particle size observed by TEM agrees well with the average crystallite size determined by XRPD. The nanostructure of the nanoparticles is shown in Fig. 3(a–c). The high-resolution TEM (HRTEM) images exhibit well defined lattice fringes of individual particles confirming their crystalline nature. Defects in the crystal structure are also observed (Fig. 3(b) and (c)).

Zero-field-cooled (ZFC) and field-cooled (FC) measurements were performed on the sample in the applied magnetic field of 100 Oe and in the temperature range of 2–300 K (Fig. 4). The FC

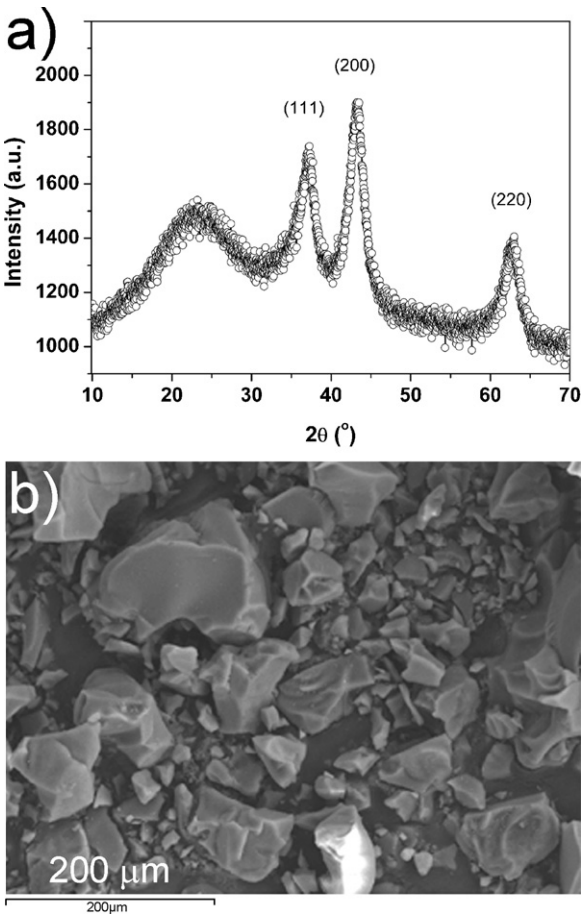

Fig. 1. (a) X-ray diffraction pattern of the NiO nanoparticles in an amorphous silica matrix. The Miller indices ($h\,k\,l$) of the peaks are also shown. (b) SEM image of the sample.

magnetization shows a continuous increase upon lowering the temperature thus showing non-interacting or weak interacting particles [22,28]. The ZFC curve shows two peaks, one sharp and narrow at ~6.5 K and another broad one at ~64 K (insets of Fig. 4). Similar behavior has been found in NiO nanoparticles, and was interpreted as freezing temperature (lower peak) and blocking temperature (higher peak) [21–23,26–28].

Fig. 5 shows the field dependence in the ±5 T range of magnetization at 2 K, 5 K, 10 K and 40 K. The sample was cooled in zero fields from the room temperature to the measurement temperatures. Then, the data were taken while the magnetic field was raised to 5 T (initial curve), then decreased to −5 T (demagnetization curve), and then again increased to 5 T (remagnetization curve). The obtained values of the coercivity, remanent magnetization and saturation magnetization (Fig. 5) are given in Table 1. The values of M_S were determined by extrapolating M to infinite magnetic field. Both at 2 K and 5 K, the hysteresis displays an anomalous behavior showing that the magnetization initial curve lies below the hysteresis loop (Fig. 5(a) and (b)). At the temperature of 10 K the anomalous

Table 1
Magnetic parameters obtained from the hysteresis loops.

Temperature [K]	H_C [Oe]	M_r [emu/g]	M_S [emu/g]	Magnetic behavior
2	285	3.71	26.65	Anomalous
5	31	0.33	28.44	Anomalous
10	60	0.041	8.9	Normal
40	53	0.013	8.49	Normal

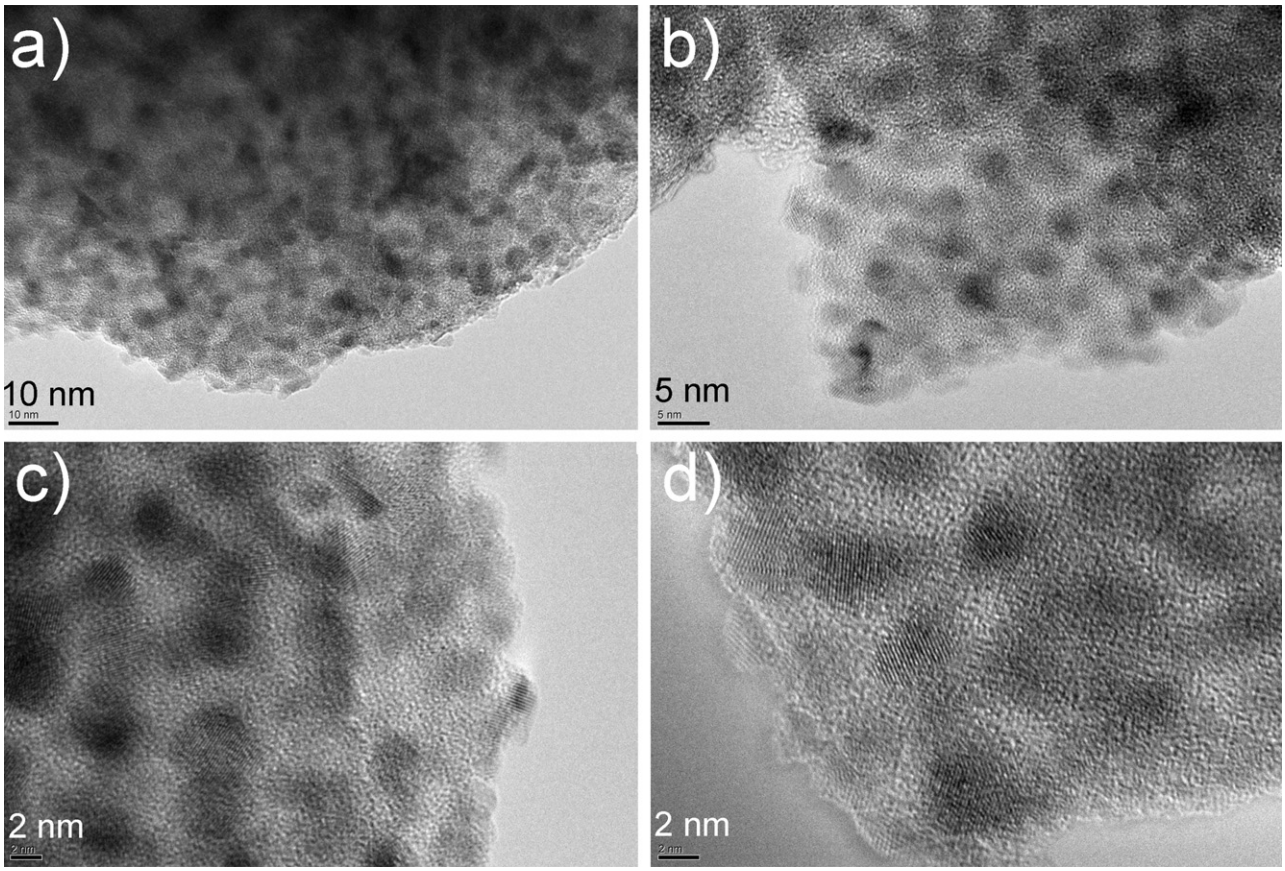

Fig. 2. TEM images of the NiO nanoparticles in an amorphous silica matrix.

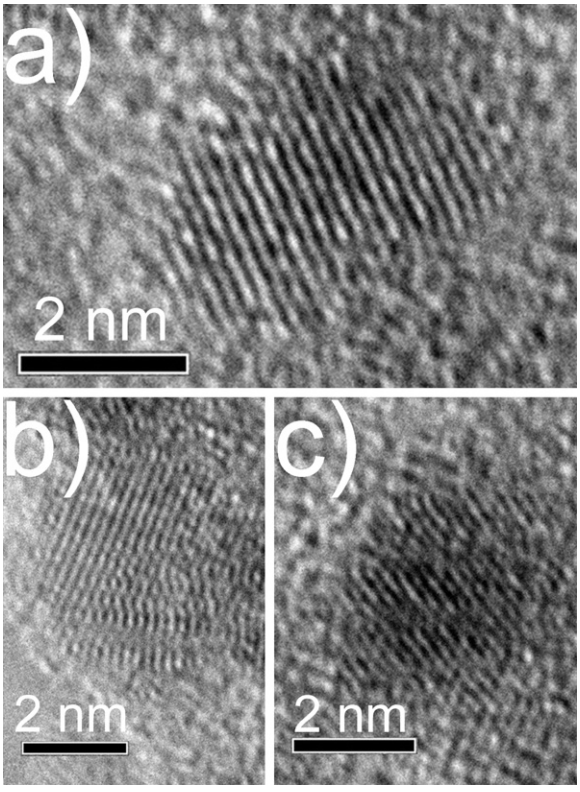

Fig. 3. HRTEM images of the NiO nanoparticles.

behavior had already disappeared and hysteretic behavior is normal (Fig. 5(c)). Normal hysteretic behavior is also observed at 40 K (Fig. 5(d)). Moreover, the initial curves do not show an S shape which is observed in systems with strong inter-particle interactions [21,22].

Finally, we discuss the possible origin of the anomalous magnetic behavior. The saturation magnetization of ~27 emu/g (at 2 K and 5 K, Table 1) is high for antiferromagnetic materials and is much bigger than the magnetization of bulk NiO materials. Moreover, high remanent magnetizations are also observed at low temperatures (Table 1). These high magnetizations (M_r and M_S) probably arise from the uncompensated surface spins which are aligned and

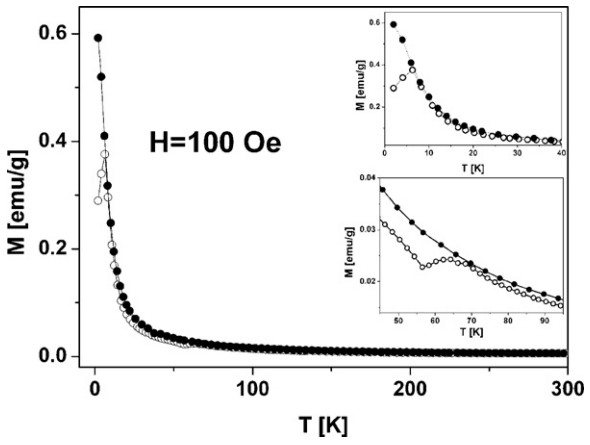

Fig. 4. Temperature dependence of the zero-field-cooled (ZFC, open symbols) and field-cooled (FC, solid symbols) magnetization measured in a field of 100 Oe.

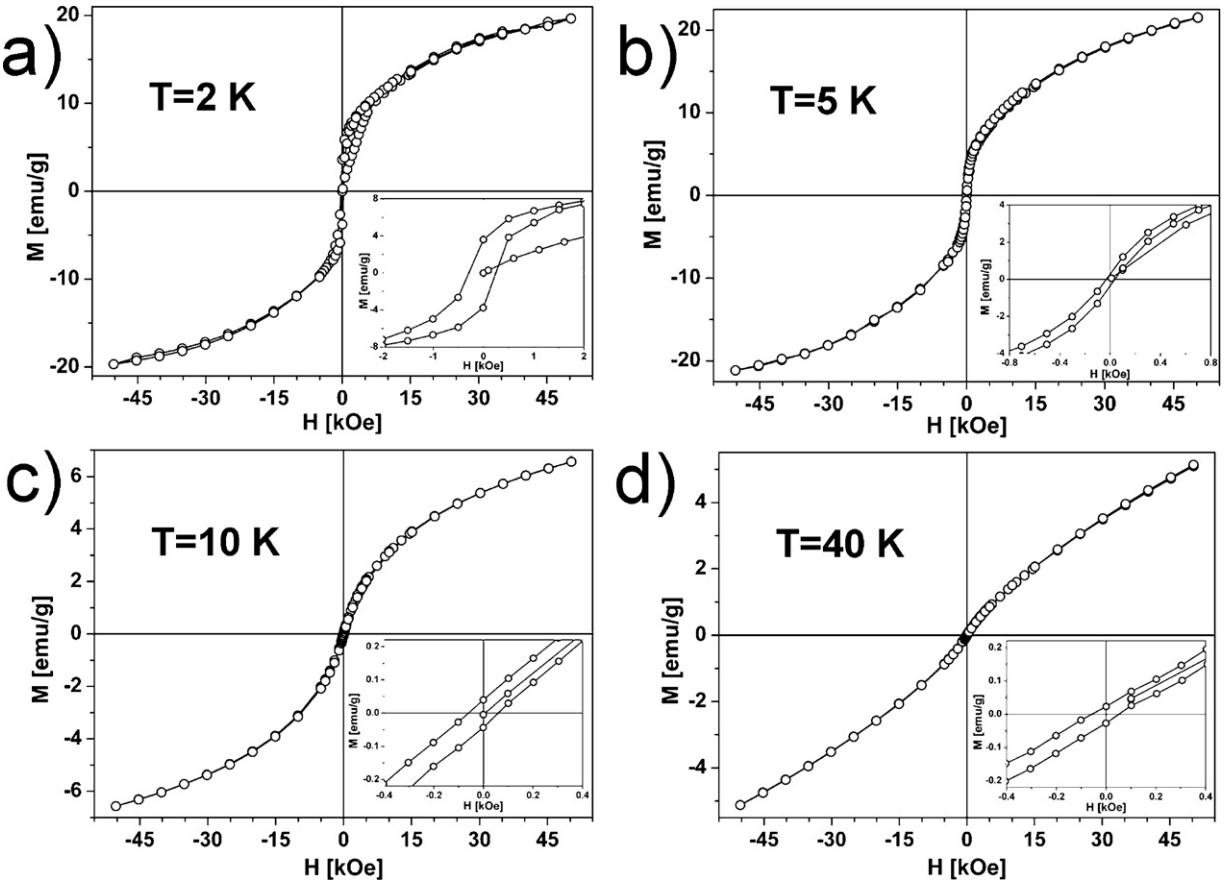

Fig. 5. Field dependence of magnetization recorded at 2 K (a), 5 K (b), 10 K (c) and 40 K (d). The insets show low field magnetization behavior.

frozen in the direction of the magnetic field at low temperatures. Moreover, the existence of non-exact compensation of spins in antiferromagnetic core is also expected to contribute to these high magnetization values (defects in particles, Fig. 3(b) and (c)) [58–60]. The M_S and M_r values are significantly smaller at higher temperatures (10 K and 40 K, Table 1) showing that the surface spins freely fluctuate (surface spins are unfrozen). After above facts, we conjecture that the NiO nanoparticle consists of magnetically disorder shell and antiferromagnetically order core with an uncompensated magnetic moment. When the sample is cooled down to temperature below 6.5 K (zero-field cooling) the surface spins freeze into a spin-glass-like configuration whereas the core spins are blocked and aligned along easy axes. The nanoparticle surface spins are exchange coupled to the core spins and part of the surface spins are aligned in the direction of the easy axes (preferred direction). In the magnetic field (initial curve) the surface spins rotate together with the core spins toward the field direction. With increasing magnetic field the number of surface spins directed along the field direction increases. The large fields orient all surface spins parallel to the field direction (Fig. 5(a), break in the initial curves $\approx$ 1 T). When this alignment is reached (field induced orientation of the surface spins), the magnetization remains increased up to the 5 T but with lower slope (smaller susceptibility) due to the core spins. With decreasing field (demagnetization curve), some of the surface spins are still aligned and frozen in the direction of the magnetic field up to the zero field (high value of the remanent magnetization, Table 1). When the magnetic field is reversed the surface spins change their direction (weak exchange interactions between surface spins) and rotate toward the reversed field direction showing sharp decrease of the magnetization. The demagnetization curve shows same behavior as initial curve in the high fields (Fig. 5). In the remagnetization curve measurements (positive part of fields), the surface spins also rotate in the field direction and provide a pinning force to the core spins. These provide sharp increase of the magnetization and higher values compared to the initial magnetization for a certain field range. With increasing temperature the number of frozen spins decreases, the surface spin effect becomes weaker and disappeared at 10 K (normal hysteresis behavior). The field dependence of the magnetizations M(H) are in agreement with the temperature dependence of the magnetization M(T) (Fig. 4), implying that the surface spins dominate the magnetic properties at low temperatures. Moreover, H_C values show random trend with temperature (Table 1). The increase of the coercivity below blocking temperature (higher maximum) with decrease of the temperature is well known for nanomaterials [61–63]. On the other hand, the decrease of the coercivity at temperatures below blocking and a sharp increase afterwards are unusual. Similar unusual behavior of H_C in NiO nanoparticles has been reported in the literature [21,22,26–28]. This behavior should also arise from the surface spin dynamics. A possible explanation is the formation of superparamagnetic surface spin clusters which can decrease surface anisotropy i.e. decrease the coercivity (around the lower maximum). Below the lower maximum surface spins are in a spin-glass-like state and lead to increases of the surface anisotropy i.e. increase of the coercivity [21,22].

4. Conclusions

The NiO nanoparticles embedded in an amorphous silica matrix have been synthesized by a sol–gel combustion method. The method provides an inexpensive and easy preparation of NiO nanoparticles embedded in a silica matrix. The XRPD, TEM and

HRTEM reveal the nanocrystalline NiO phase, spherically shaped particle morphology, nanoparticle size of about 4 nm, lattice fringes of the nanoparticles and defects in the crystal structure. The *M*(T) measurements show two maximums (ZFC curve), one sharp and narrow at low temperature ~6.5 K and an other broad one at higher temperature ~64 K. Moreover, the magnetic measurements display hysteretic behavior at 2 K, 5 K, 10 K and 40 K, as well as jump of the magnetizations at 2 K and 5 K. After above facts, we conjecture that the NiO nanoparticle consists of magnetically disorder shell and antiferromagnetically order core with an uncompensated magnetic moment. The unusual magnetism in NiO nanoparticles is also given by hysteretic behavior at 2 K and 5 K where initial magnetization curve lies below the hysteresis loop which is a novel effect in NiO systems. These anomalous behaviors are discussed as consequence of the surface spins which are frozen at low temperatures (2 K and 5 K). The origin of such anomalous behavior demands further investigation.

Acknowledgements

M.T. acknowledges Professor Veljko Dmitrasinović (Institute for Physics, Belgrade) for his comments. The Serbian Ministry of Science has supported this work financially under grant no. III 45015.

References

[1] H.B. Lu, L. Liao, J.C. Li, M. Shuai, Y.L. Liu, Appl. Phys. Lett. 92 (2008) 093102.
[2] P. Mallick, C. Rath, A. Rath, A. Banerjee, N.C. Mishra, Solid State Commun. 150 (2010) 1342.
[3] L. Barry, J.D. Holmes, D.J. Otway, M.P. Copley, O. Kazakova, M.A. Morris, J. Phys.: Condens. Matter 22 (2010) 076001.
[4] S. Bhattacharya, S. Banerjee, D. Chakravorty, J. Phys. D: Appl. Phys. 42 (2009) 095002.
[5] A.S. Bhatt, D.K. Bhat, C.-W. Tai, M.S. Santosh, Mater. Chem. Phys. 125 (2011) 347.
[6] T. Chatterji, Y. Su, G.N. Iles, Y.C. Lee, A.P. Khandhar, K.M. Krishnan, J. Magn. Magn. Mater. 322 (2010) 3333.
[7] A. Zelenakova, J. Kovac, V. Zelenak, J. Appl. Phys. 108 (2010) 034323.
[8] M.J. Benitez, O. Petracic, H. Tuyuz, F. Schuth, H. Zabel, Europhys. Lett. 88 (2009) 27004.
[9] J. Nogués, J. Sort, V. Skumryev, S. Surinach, J.S. Munoz, M.D. Baró, Phys. Rep. 422 (2005) 65.
[10] H. Pang, Q. Lu, Y. Li, F. Gao, Chem. Commun. (2009) 7542.
[11] A.M. Zhang, H.L. Cai, X.S. Wu, J. Supercond. Nov. Magn. 23 (2010) 863.
[12] Y. Ding, Y. Wang, L. Su, H. Zhang, Y. Lei, J. Mater. Chem. 20 (2010) 9918.
[13] S. Gandhi, N. Nagalakshmi, I. Baskaran, V. Dhanalakshmi, M.R. Gopinathan Nair, R. Anbarasan, J. Appl. Polym. Sci. 118 (2010) 1666.
[14] K.L. Zhou, F. Gu, C.Z. Li, J. Alloys Compd. 474 (2009) 358.
[15] M.F. Hassan, M.M. Rahman, Z. Guo, Z. Chen, H. Liu, J. Mater. Chem. 20 (2010) 9707.
[16] H. Steinebach, S. Kannan, L. Rieth, F. Solzbacher, Sens. Actuators B: Chem. 151 (2010) 162.
[17] J. Xu, L. Gao, J. Cao, W. Wang, Z. Chen, J. Solid State Electrochem. (2010), doi:10.1007/s10008-010-1222-6.
[18] G. Srinivasan, M. Seehra, Phys. Rev. B 29 (1984) 6295.
[19] M.S. Seehra, P. Dutta, H. Shim, A. Manivannan, Solid State Commun. 129 (2004) 721.
[20] S.D. Tiwari, K.P. Rajeev, Phys. Rev. B 72 (2005) 104433.
[21] E. Winkler, R.D. Zysler, M.V. Mansilla, D. Fiorani, Phys. Rev. B 72 (2005) 132409.
[22] E. Winkler, R.D. Zysler, M.V. Mansilla, D. Fiorani, D. Rinaldi, M. Vasilakaki, K.N. Trohidou, Nanotechnology 19 (2008) 185702.
[23] M. Jagodič, Z. Jagličić, A. Jelen, J.B. Lee, Y.M. Kim, H.J. Kim, J. Dolinšek, J. Phys.: Condens. Matter 21 (2009) 215302.
[24] R.H. Kodama, S.A. Makhlouf, A.E. Berkowotz, Phys. Rev. Lett. 79 (1997) 1393.
[25] J.B. Yi, J. Ding, Y.P. Feng, G.W. Peng, G.M. Chow, Y. Kawazoe, B.H. Liu, J.H. Yin, S. Thongmee, Phys. Rev. B 76 (2007) 224402.
[26] N.M. Carneiro, W.C. Nunes, R.P. Borges, M. Godinho, L.E. Fernandez-Outon, W.A.A. Macedo, I.O. Mazali, J. Phys. Chem. C 114 (2010) 18773.
[27] M.Y. Ge, L.Y. Han, U. Wiedwald, X.B. Xu, C. Wang, K. Kuepper, P. Ziemann, J.Z. Jiang, Nanotechnology 21 (2010) 425702.
[28] C.T. Meneses, J.G.S. Duque, E. de Biasi, W.C. Nunes, S.K. Sharma, M. Knobel, J. Appl. Phys. 108 (2010) 013909.
[29] S. Vaidya, K.V. Ramanujachary, S.E. Lofland, A.K. Ganguli, Cryst. Growth Des. 9 (2009) 1666.
[30] M. Tadić, M. Panjan, D. Marković, Mater. Lett. 64 (2010) 2129.
[31] S. Mandal, S. Banerjee, K.S.R. Menon, Phys. Rev. B 80 (2009) 214420.
[32] S.K. Sharma, J.M. Vargas, E. de Biasi, F. Beron, M. Knobel, K.R. Pirota, C.T. Meneses, S. Kumar, C.G. Lee, P.G. Pagliuso, C. Rettori, Nanotechnology 21 (2010) 035602.
[33] S.A. Makhlouf, H. Al-Attar, R.H. Kodama, Solid State Commun. 145 (2008) 1.
[34] V. Bisht, K.P. Rajeev, J. Phys.: Condens. Matter 22 (2010) 016003.
[35] K. Karthik, G.K. Selvan, M. Kanagaraj, S. Arumugam, N.V. Jaya, J. Alloys Compd. 509 (2011) 181.
[36] M. Casu, A. Lai, A. Musinu, G. Piccaluga, S. Solinas, S. Bruni, F. Cariati, E. Beretta, J. Mater. Sci. 36 (2001) 3731.
[37] Y. Wu, Y. He, T. Wu, T. Chen, W. Weng, H. Wan, Mater. Lett. 61 (2007) 3174.
[38] Q. Yang, J. Sha, X. Ma, D. Yang, Mater. Lett. 59 (2005) 1967.
[39] Z. Wei, H. Qiao, H. Yang, C. Zhang, X. Yan, J. Alloys Compd. 479 (2009) 855.
[40] E.R. Beach, K. Shqau, S.E. Brown, S.J. Rozeveld, P.A. Morris, Mater. Chem. Phys. 115 (2009) 371.
[41] F. Davar, Z. Fereshteh, M.S. Niasari, J. Alloys Compd. 476 (2009) 797.
[42] L. Bai, F. Yuan, P. Hu, S. Yan, X. Wang, S. Li, Mater. Lett. 61 (2007) 1698.
[43] Y. Wu, Y. He, T. Wu, W. Weng, H. Wan, Mater. Lett. 61 (2007) 2679.
[44] S. Manna, A.K. Deb, J. Jagannath, S.K. De, J. Phys. Chem. C 112 (2008) 10659.
[45] Y.Z. Zheng, M.L. Zhang, Mater. Lett. 61 (2007) 3967.
[46] N. Srivastava, P.C. Srivastava, Phys. E 42 (2010) 2225.
[47] S.F. Wang, L.Y. Shi, X. Feng, S.R. Ma, Mater. Lett. 61 (2007) 1549.
[48] A.M. Reddy, A.S. Reddy, P.S. Reddy, Mater. Chem. Phys. 125 (2011) 434.
[49] M. Tadić, D. Marković, V. Spasojević, V. Kusigerski, M. Remškar, J. Pirnat, Z. Jagličić, J. Alloys Compd. 441 (2007) 291.
[50] V. Zelenak, A. Zelenakova, J. Kovac, U. Vainio, N. Murafa, J. Phys. Chem. C 113 (2009) 13045.
[51] M. Tadic, V. Kusigerski, D. Markovic, I. Milosevic, V. Spasojevic, J. Magn. Magn. Mater. 321 (2009) 12.
[52] A. Kamyabi-Gol, S.M. Zebarjad, S.A. Sajjadi, Colloids Surf. A 336 (2009) 69.
[53] V.I. Bakhmutov, B.G. Shpeizer, A.V. Prosvirin, K.R. Dunbar, A. Clearfield, Microporous Mesoporous Mater. 118 (2009) 78.
[54] D. Buso, M. Guglielmi, A. Martucci, C. Cantalini, M.L. Post, A. Hache, J. Sol–Gel Sci. Technol. 40 (2006) 299.
[55] J. Zong, Y. Zhu, X. Yang, C. Li, J. Alloys Compd. 509 (2011) 2970.
[56] E.D. Gaspera, D. Buso, M. Guglielmi, A. Martucci, V. Bello, G. Mattei, M.L. Post, C. Cantalini, S. Agnoli, G. Granozzi, A.Z. Sadek, K. Kalantar-zadeh, W. Wlodarski, Sens. Actuators B: Chem. 143 (2010) 567.
[57] S.R. Lukić, D.M. Petrović, M.D. Dramićanin, M. Mitrić, L.J. Đačanin, Scr. Mater. 58 (2008) 655.
[58] J.T. Richardson, D.I. Yiagas, B. Turk, K. Forster, M.V. Twigg, J. Appl. Phys. 70 (1991) 6977.
[59] S.A. Makhlouf, F.T. Parker, F.E. Spada, A.E. Berkowitz, J. Appl. Phys. 81 (1997) 5561.
[60] L. Néel, C. R Acad. Sci. Paris 252 (1961) 4075.
[61] P. Gorria, M.P. Fernandez-Garcia, M. Sevilla, J.A. Blanco, A.B. Fuertes, Phys. Status Solidi (RRL) 3 (2009) 4–6.
[62] V. Sreeja, P.A. Joy, Mater. Res. Bull. 42 (2007) 1570–1576.
[63] J.R. Jeong, S.J. Lee, J.D. Kim, S.C. Shin, Phys. Status Solidi 241 (2004) 1593–1596.